World Academy of Science, Engineering and Technology
International Journal of Electrical and Computer Engineering
Vol:12, No:9, 2018

Five-Phase Induction Motor Drive System Driven by Five-Phase Packed U Cell Inverter: Its Modeling and Performance Evaluation

Mohd Tariq

***Abstract*—**The three phase system drives produce the problem of more torque pulsations and harmonics. This issue prevents the smooth operation of the drives and it also induces the amount of heat generated thus resulting in an increase in power loss. Higher phase system offers smooth operation of the machines with greater power capacity. Five phase variable-speed induction motor drives are commonly used in various industrial and commercial applications like tractions, electrical vehicles, ship propulsions and conveyor belt drive system. In this work, a comparative analysis of the different modulation schemes applied on the five-level five-phase Packed U Cell (PUC) inverter fed induction motor drives is presented. The performance of the inverter is greatly affected with the modulation schemes applied. The system is modeled, designed, and implemented in MATLAB®/Simulink environment. Experimental validation is done for the prototype of single phase, whereas five phase experimental validation is proposed in the future works.

***Keywords*—**Packed U-Cell inverter, pulse width modulation, five-phase system, induction motor.

I. Introduction

SQUIRREL cage induction motors (SCIMs) are widely used motors in industries and commercial applications. IM has replaced the DC machines in drives application since last century. The strong features of induction machines include ruggedness, commutation less, low cost and similar characteristics of DC motor by using vector control. For variable speed application although it has complex control, but advancement of the microprocessors and microcontrollers has vanished this limitation and it is easier to implement now a days [1].

By introducing the multiphase system, amplitude of the torque pulsation can be reduced and it also ensures the good performance of the of the electro-mechanical system of the inverter fed motor drives even at reduced load. Multiphase system concept, inverters of large power ratings can be easily realized with lower rating of switches because the power handled by one leg is reduced as number of phase increases. It is also realized that overall performance of higher order phase system is better as compared to traditional three phase system drives. Multiphase system drives exhibit a better fault tolerance capability [2].

When a five-phase IM is supplied by ten-step voltage source inverter, the amplitude of torque pulsations get reduced by one third and frequency increases, hence the improvement reported in literature is that a severe distortion in the input side current is resolved by choosing proper modulation schemes in multiphase VSI [3]. The multiphase drives concept is limited in drives application only because of requirement of the high number of the active and passive device counts that increases the inverter complexity. Five-phase and six-phase drives are more common in application and discussed in detail in [4], [5]. In [5], authors have optimized the performance of five-phase motor drives with considerable improvement in torque pulsation at the cost of complex mathematical control using sliding mode control.

The main aspect of this presented work is to implement the five-phase induction motor drive fed by the five phase five level PUC inverter with different carrier based PWM schemes and to compare the performance of the modeled IM. A mathematical equation based Simulink model of the IM has been derived from the theoretical studies.

Mohd Tariq is with the Aligarh Muslim University, India (e-mail: tariq.iitkgp@gmail.com).

II. Three Phase and Five Phase System

A. Three Phase Voltage, Current and Power Relation

Fig. 1 shows the phasor diagram of the three phase system. V_{an}, V_{bn} *and* V_{cn} are the phase voltage equally spaced by 120^0 and has the same magnitude. Line voltage $V_L = \sqrt{3}\, V_{ph}$ *and* $I_L = I_{ph}$. The per phase power is $P = V_{ph} I_{ph} cos\emptyset$, and total power is sum of all phases power. In balanced condition total power $P = \sqrt{3}\, V_L I_L cos\emptyset$ or $P = 1.732\, V_L I_L cos\emptyset$.

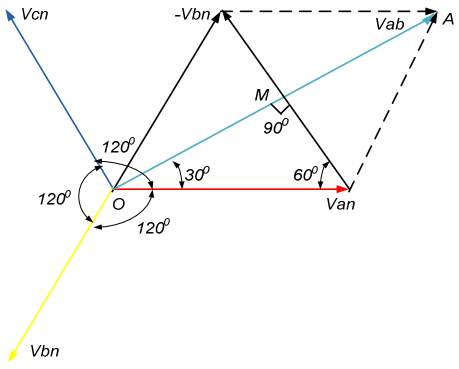

Fig. 1 Phasor diagram of three phase system

B. Five-Phase Voltage, Current and Power Relation

Fig. 2 shows the phasor diagram of the five-phase system. $V_{an}, V_{bn}, V_{cn}, V_{dn}, and\ V_{en}$ are the phase voltage equally spaced by 72^0 and have an equal magnitude. The relation between line

and phase voltage is given by:

$$V_L = \sqrt{1.38}\, V_{ph} \text{ or } V_L = 1.175 V_{ph} \;\; and \;\; I_L = I_{ph}$$

Per phase, power $P = V_{ph} I_{ph} cos\emptyset$ and total power is sum of the power in each phase.

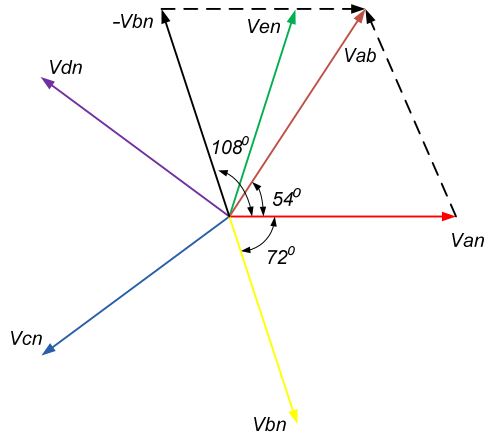

Fig. 2 Phasor diagram of five phase systems

$$P = 5 V_{ph} I_{ph} cos\emptyset \quad \text{or } P = 4.25 V_L I_L cos\emptyset$$

C. Comparison between Three Phase & Five Phase System

Three phase voltage relation:

$$V_L = \sqrt{3} V_{ph} \; or \; V_L = 1.732 V_{ph}$$

Five phase voltage relation:

$$V_L = \sqrt{1.38} V_{ph} \; or \; V_L = 1.174 V_{ph}$$

Three phase current relation:

$$I_L = I_{ph}$$

Five phase current relation:

$$I_L = I_{ph}$$

Three phase power in balance system:

$$P = \sqrt{3} V_L I_L cos\emptyset \;\; or \;\; P = 1.732 V_L I_L cos\emptyset$$

Five phase power in balance system:

$$P = 5 V_{ph} I_{ph} cos\emptyset \;\; or \;\; P = 4.25 V_L I_L cos\emptyset$$

From the above relation, we can conclude that, in five-phase system, line voltage is 1.47 time less than the three-phase system. But, the power capacity is 2.52 times more than the three phase system for the same phase voltage [6].

III. Five Phase Five Level PUC Inverter and Mudlation Techniques

The power circuit structure of the PUC inverter is shown in Fig. 3. It comprises of six switches $T_1, T_2, T_3\; T_4, T_5 \; and \; T_6$. Among them, there are three pairs $(T_1, T_4), (T_2, T_5) \; and \; (T_3, T_6)$. Each pair is working in complementary. V_1 is the separate DC source voltage, and V_C is the capacitor voltage which is to be maintained to generate the required number of levels [7]. Fig. 4 shows the five-phase five level PUC inverter.

This circuit is able to generate five level and seven level output by varying the capacitor voltage. For five-level capacitor, voltage should be maintained at one half of DC source voltage [8].

$$\begin{bmatrix} \frac{di_L}{dt} \\ \frac{dV_2}{dt} \end{bmatrix} = \begin{bmatrix} \frac{-R_f}{L_f} i_L - \frac{V_L}{L_f} \\ 0 \end{bmatrix} + \begin{bmatrix} \frac{V_1}{L_f} & \frac{V_1 - V_2}{L_f} & \frac{-V_2}{L_f} \\ 0 & \frac{-i_L}{C} & \frac{i_L}{C} \end{bmatrix} \begin{bmatrix} d_1 \\ d_2 \\ d_3 \end{bmatrix} \qquad (1)$$

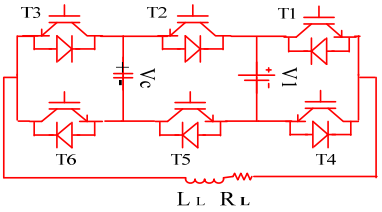

Fig. 3 Single phase PUC inverter

TABLE I
PUC Inverter Switching Table

States	T_1	T_2	T_3	Output
1	1	0	0	V_1
2	1	0	1	V_1-V_c
3	1	1	0	V_c
4	1	1	1	0
5	0	0	0	0
6	0	0	1	-V_c
7	0	1	0	V_c-V_1
8	0	1	1	-V_1

Equation (1) shows the state space model of the PUC inverter. Many modulation techniques are found in the literature for the multilevel multiphase inverter. Carrier based PWM schemes is found on two-level five-phase inverter [9], [10]. The control and modulation algorithm of the proposed PUC fed IM drives must meet the following requirements [11]:

- The variations in DC input voltage must be managed.
- The output voltage of inverter must be regulated.
- Constant volts and frequency control requirements must be met [11].

In order to achieve an improved harmonic profile and an increased output voltage, the PWM method has been applied for AC drives [12].

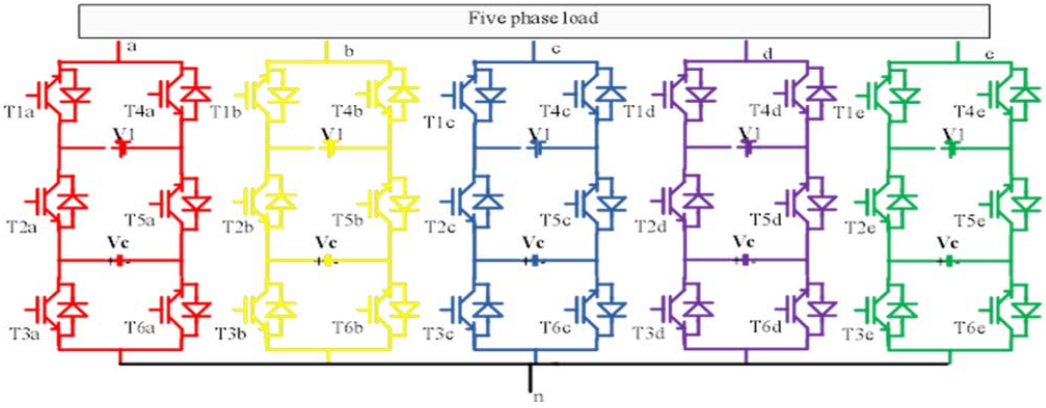

Fig. 4 Five-phase five-level inverter

$$F(t) = \frac{MV}{2}\cos(\omega_F t) + \frac{2V}{\pi}\sum_{m=1}^{\infty} J_o(mM\frac{\pi}{2})\sin(m\frac{\pi}{2}) .\cos(m\omega_c t) + \frac{2V}{\pi}\sum_{m=1}^{\infty}\sum_{n=1}^{\pm\infty}\frac{J_n\frac{mM\pi}{2}}{m} * *sin\left((m+n)\frac{\pi}{2}\right)cos(m\omega_c + n\omega_F t) \quad (2)$$

where M= modulation index, ω_c = freq. of carrier (rad/sec) ω_F= freq. of fundamental (reference), V= supply voltage (V) J_o, J_n = Bessel function of first kind.

Equation (2) comprises three terms:

a) First term gives the amplitude of fundamental component which is proportional to modulation index M.
b) Second term shows amplitude of the harmonics content at the carrier and multiple of the carrier frequency.
c) Third term gives the amplitude of harmonics at side band.

IV. Five Phase IM Model

Five-phase IM is modeled using the mathematical equation of voltage, current and torque that presents the dynamic behavior of IM. A multiphase winding is reduced into set of two winding (d-q) which are quadrature to each other. Five-phase winding of the IM under balanced condition can be expressed by (3) [13]:

$$\left.\begin{aligned} V_a &= \sqrt{2}V_{rms}\sin(\omega_t) \\ V_b &= \sqrt{2}V_{rms}\sin(\omega_t - \frac{2\pi}{5}) \\ V_c &= \sqrt{2}V_{rms}\sin(\omega_t - \frac{4\pi}{5}) \\ V_d &= \sqrt{2}V_{rms}\sin(\omega_t + \frac{4\pi}{5}) \\ V_e &= \sqrt{2}V_{rms}\sin(\omega_t + \frac{2\pi}{5}) \end{aligned}\right\} \quad (3)$$

This five-phase model is transferred into d-q-o variables by transformation matrix, the decoupling transformation matrix can be expressed by (4):

$$\begin{bmatrix} V_d \\ V_q \\ V_x \\ V_y \\ V_0 \end{bmatrix} = \frac{2}{5}\begin{bmatrix} 0 & -\sin\alpha & -\sin 2\alpha & -\sin 3\alpha & -\sin 4\alpha \\ 1 & \cos\alpha & \cos 2\alpha & \cos 3\alpha & \cos 4\alpha \\ 1 & \cos 3\alpha & \cos 6\alpha & \cos 9\alpha & \cos 12\alpha \\ 0 & -\sin 3\alpha & -\sin 6\alpha & -\sin 9\alpha & -\sin 12\alpha \\ 0.5 & 0.5 & 0.5 & 0.5 & 0.5 \end{bmatrix}\begin{bmatrix} V_a \\ V_b \\ V_c \\ V_d \\ V_e \end{bmatrix} \quad (4)$$

where $\alpha = \frac{2\pi}{5}$

The nature of this equation is similar to the three-phase induction machine equations, the model of five phase induction machine with stator side voltage equation in d-q and q- reference is given by [14]:

$$\left.\begin{aligned} V_{ds} &= R_s i_{ds} - \omega_a \emptyset_{qs} + p\emptyset_{ds} \\ V_{qs} &= R_s i_{qs} + \omega_a \varphi_{ds} + p\varphi_{qs} \\ V_{xs} &= R_s i_{xs} + p\varphi_{xs} \\ V_{ys} &= R_s i_{ys} + p\varphi_{ys} \\ V_{os} &= R_s i_{os} + p\varphi_{os} \end{aligned}\right\} \quad (5)$$

Rotor side voltage equation in d-q and q- reference frame is given as:

$$\left.\begin{aligned} V_{dr} &= R_r i_{dr} - (\omega_a - \omega)\varphi_{qr} + p\varphi_{dr} \\ V_{qr} &= R_r i_{qr} + (\omega_a - \omega)\varphi_{dr} + p\varphi_{qr} \\ V_{xr} &= R_r i_{xr} + p\varphi_{xr} \\ V_{yr} &= R_r i_{yr} + p\varphi_{yr} \\ V_{0r} &= R_r i_{or} + p\varphi_{or} \end{aligned}\right\} \quad (6)$$

Flux equation of stator side of five-phase IM can be given by:

$$\left.\begin{aligned} \varphi_{qs} &= (L_{ls} + L_m)i_{ds} + L_m i_{dr} \\ \varphi_{ds} &= (L_{ls} + L_m)i_{qs} + L_m i_{qr} \\ \varphi_{xs} &= L_{ls} i_{xs} \\ \varphi_{ys} &= L_{ls} i_{ys} \\ \varphi_{os} &= L_{ls} i_{os} \end{aligned}\right\} \quad (7)$$

Flux equation of rotor side of five phase IM can be given by:

$$\left.\begin{aligned} \varphi_{qr} &= (L_{lr} + L_m)i_{dr} + L_m i_{ds} \\ \varphi_{dr} &= (L_{ls} + L_m)i_{qr} + L_m i_{qs} \\ \varphi_{xr} &= L_{lr} i_{xr} \\ \varphi_{yr} &= L_{lr} i_{yr} \\ \emptyset_{or} &= L_{lr} i_{or} \end{aligned}\right\} \quad (8)$$

where $L_m = (n/2)M$, and M is the peak value of mutual

inductance. R and L hold the resistance and inductance, v, i *and* $\emptyset$ represent voltage, current and flux linkage respectively, and l shows leakage inductance. Torque and speed equation is given by (9).

$$\left.\begin{aligned} T_e &= \frac{5}{2}\left(\frac{P}{2}\right)\frac{1}{\omega_b}\left(\varphi_{ds} i_{qs} - \omega_{qs} i_{ds}\right) \\ \omega_r &= \int \frac{P}{2J}\left(T_e - T_L\right) \end{aligned}\right\} \quad (9)$$

where, P is the number of poles, J is the moment of inertia, T_L is the load torque, T_e is the machine torque, and ω_r is the rotor speed. This model is the same as the three phase machine model, the only difference is due to presence of x-y components in voltage and flux equation. Due to being shorted of rotor bars/windings x-y components does not appear in the rotor windings. When the voltage applied to the stator windings V_a, V_b, V_c, V_d and V_e is transformed to d-q reference frame then flux linkage, torque, speed and current equations can be implemented. To obtain the current in terms of i_{qs}, i_{ds},i_{qr} and i_{dr}, inverse transformation equations are used to get the stator currents in machine variable form.

$$\begin{bmatrix} i_{as} \\ i_{bs} \\ i_{cs} \\ i_{ds} \\ i_{es} \end{bmatrix} = \sqrt{\frac{2}{5}} \begin{bmatrix} 1 & 0 & 1 & 0 & 1 \\ \cos\alpha & \sin\alpha & \cos 2\alpha & \sin 2\alpha & 1 \\ \cos 2\alpha & \sin 2\alpha & \cos 4\alpha & \sin 4\alpha & 1 \\ \cos 3\alpha & \sin 3\alpha & \cos 6\alpha & \sin 6\alpha & 1 \\ \cos 4\alpha & \sin 4\alpha & \cos 8\alpha & \sin 8\alpha & 1 \end{bmatrix} \begin{bmatrix} i_{ds} \\ i_{qs} \\ i_{xs} \\ i_{ys} \\ i_{0s} \end{bmatrix} \quad (10)$$

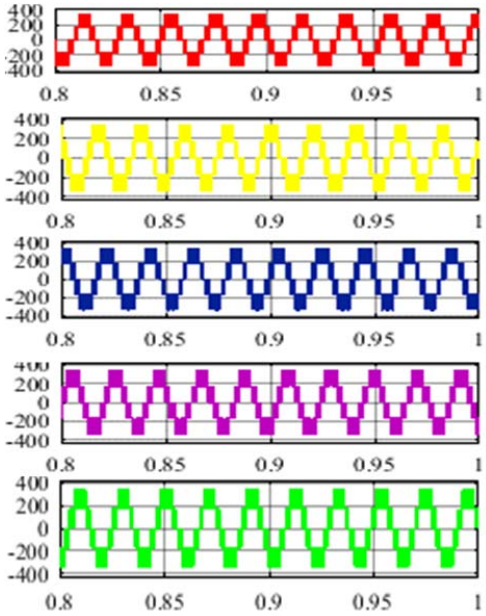

Fig. 5 Five phase voltage of PUC inverter

The produced five-phase voltage by the PUC inverter which is expressed by (3) is shown in Fig. 5, and the transformed d-q axis stator voltage expressed by (4) is shown in Fig. 6, these two voltages are quadrature in phase as can be seen by Fig. 6.

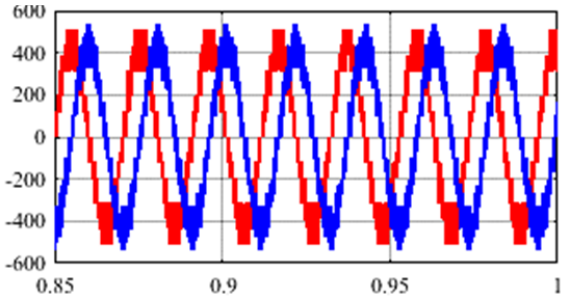

Fig. 6 d and q-axis stator voltage

V. Performance of the System under Different Modulation Schemes

The system is modeled for two modulation schemes one for triangular carrier waves and other for sawtooth carrier waves. The line voltage is taken as 320 V. The simulation work is performed for implementing the closed loop constant *v/f* control. Table II represents the simulation parameters.

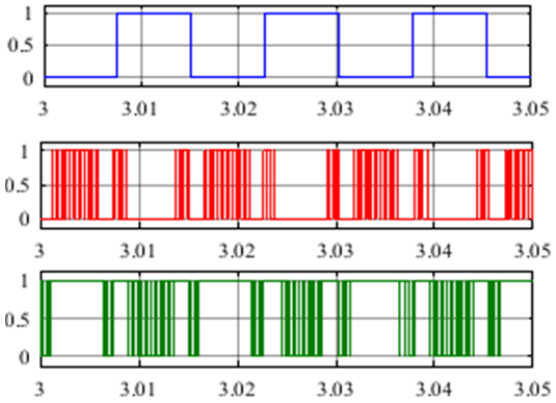

Fig. 7 Switching signal to IGBT

A. Performance under Triangular In-Phase Disposition Pwm Scheme

The simulation is first performed for triangular carrier waves in IPD-PWM schemes. For five phases, four carrier waves are used, which are vertically spaced [15].

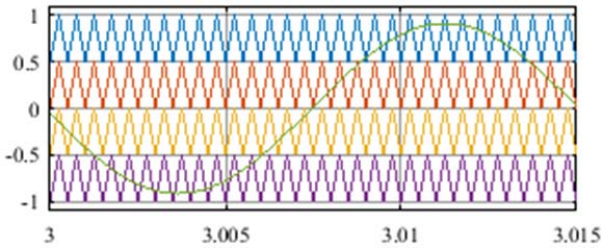

Fig. 8 Reference and triangular carrier waves

The initial reference speed is given as776 rpm at t=0.5 s. Then, the reference speed is changed to 880 rpm at t=1.52 s. Again, the reference speed is increased to 1164 rpm at t=2.2 s, and finally the reference speed is increased to 1360 rpm at t=3.0 s. The actual speed is following the reference speed very well. The speed-time characteristics under no load condition

are shown in Fig. 9.

The steady state waveform of the stator current is shown in Fig. 10. At the time of starting, an inrush current is drawn from the inverter, but after a few cycles steady state condition is arrived. Initially machine torque is increasing due to heavy inrush current, but steady state condition is achieved shortly after few cycles. Fig. 11 shows the no-load torque characteristics. After t=0.8 s, steady state condition is achieved, and torque comes to zero because of no load.

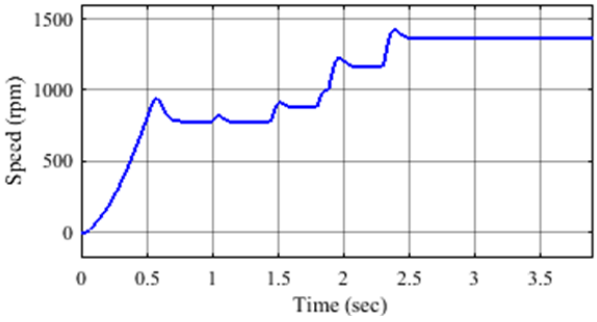

Fig. 9 Speed response for open-loop constant *v/f* control at no-load

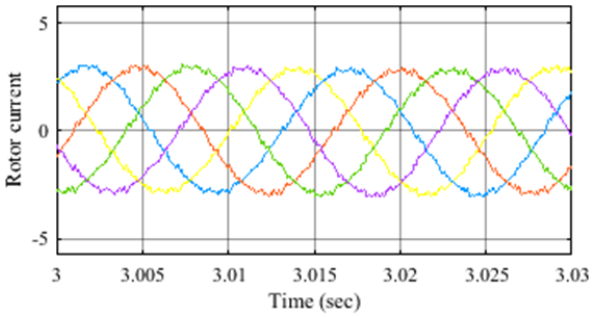

Fig. 10 Stator current at steady state

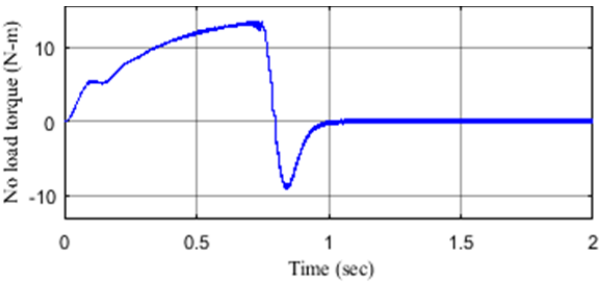

Fig. 11 No load electromagnetic torque

B. Performance under Sawtooth Phase Disposition PWM Scheme

It is similar to the triangular IPD-PWM scheme; except that, triangular waves are replaced by sawtooth wave as shown in Fig. 12.

The initial reference speed is given 776 rpm at t=0.5 s, then the reference speed is changed to 880 rpm at t=1.52 s. Again, the reference speed is increased to 1164 rpm at t=2.2 s, and finally, the reference speed is increased to 1360 rpm at t=3.0 s. The actual speed is following the reference speed very well. The speed-time characteristics under no load condition are shown in Fig. 13.

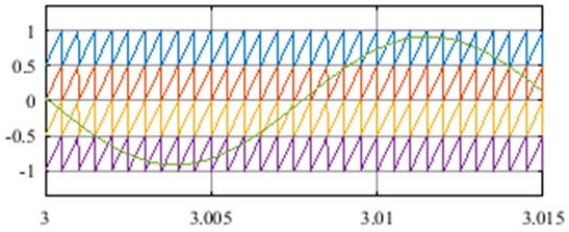

Fig. 12 Reference and sawtooth carrier waves

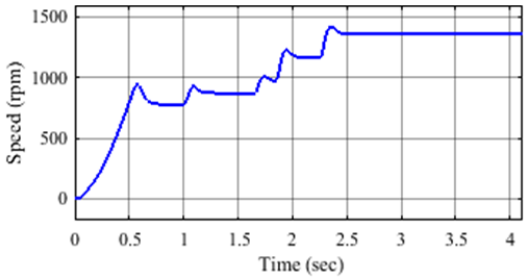

Fig. 13 Speed response for open-loop constant *v/f* control at no-load

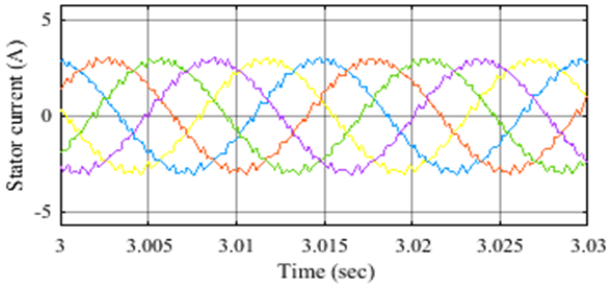

Fig. 14 Stator current at steady state

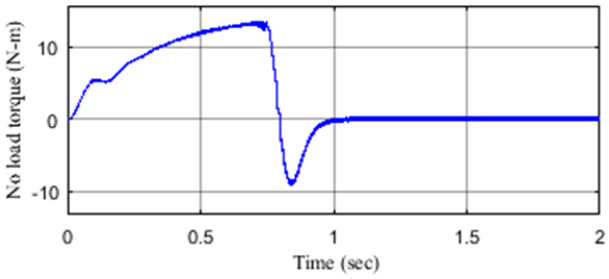

Fig. 15 No-load electromagnetic torque

TABLE II
SIMULATION PARAMETERS

Particulars	Values
Stator windings resistance	10 Ω
Rotor side resistance	6.3 Ω
Leakage inductance at stator side	0.46 H
Leakage inductance at rotor side	0.46 H
Mutual inductance	0.40 H
Number of poles	4
Inverter DC link voltage	340 V
Auxiliary DC link capacitor	4.7 mF
Switching frequency	2 kHz
System frequency	50 Hz

The steady state waveform of the stator current is shown in Fig. 14. At the time of starting, an inrush current is drawn from the inverter but after a few cycles steady state condition is arrived. Fig. 15 shows the no-load torque characteristics. After t=0.8 s, steady state condition is achieved and torque comes to zero because of no load.

VI. Experimental Validation and Future Works

The experimental validation is performed for single phase PUC inverter on a DSP TMS320F28335 development board in the laboratory as shown in Fig. 16. The simulation model of the system is burned into hex code, and that hex code is loaded on the DSP board with the Code Composer Studio version 5(CCSv5). The PWM signal is appropriately generated to switch the power IGBT (FGA25N120ANTD). The output of the DSP is just 3.3 V which is not able to turn on the IGBT, hence to boost the gating signal to 12-Volt isolated driver circuit using TLP250 is used.

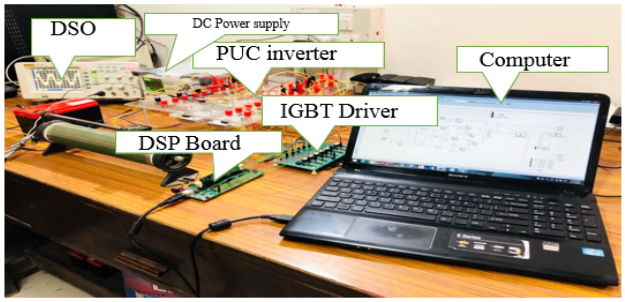

Fig. 16 Experimental prototype setup

The boosted gating signal is given to the IGBT. For experimental validation, V= 26 DC Volts is taken, and requirement of auxiliary DC link is fulfilled by using an electrolytic capacitor of 4.7 mF. The sensing of the voltage and current is implemented successfully. The model is developed for powerline frequency 50 Hz.

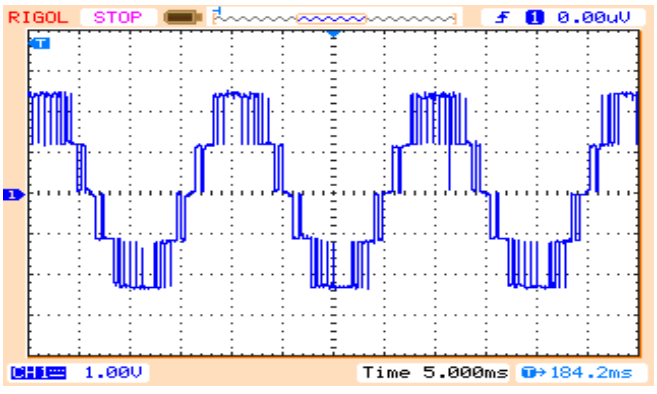

Fig. 17 Output result (waveform is scaled by 10)

Experimental result for single phase PUC inverter is shown in Fig. 17, wherein the waveform is scaled by a factor of 10. The proposed experimental validation of the five-phase PUC inverter fed by five-phase induction machine is planned for the future work, and if the results are obtained before the camera ready paper submission, we may include the final experimental results in the manuscript.

VII. Conclusion

The aim of this paper was to model and simulate the behavior of five-phase PUC fed by five-phase IM operated drive. The mathematical model was derived and was implemented for constant *v/f* speed control under different carrier based PWM schemes. The simulation model is performed successfully in MATLAB®/Simulink environment. In both carrier-based modulation scheme, the torque-time characteristics are similar but speed characteristics in triangular carrier-based scheme are smoother, and also, stator current has less ripple in triangular carrier scheme. Based on these results, triangular PWM scheme has been recommended for these drive applications.

References

[1] R. H. Kumar, A. Iqbal, and N. C. Lenin, "Review of recent advancements of direct torque control in induction motor drives – a decade of progress," *IET Power Electron.*, vol. 11, no. 1, pp. 1–15, Jan. 2018.

[2] Z. Wang, X. Wang, Y. Wang, J. Chen, and M. Cheng, "Fault Tolerant Control of Multiphase Multilevel Motor Drives – Technical Review," vol. 3, no. 2, 2017.

[3] K. N. Pavithran, R. Parimelalagan, and M. R. Krishnamurthy, "Studies On Inverter-Fed Five-Phase Induction Motor Drive," *IEEE Trans. Power Electron.*, vol. 3, no. 2, pp. 224–235, 1988.

[4] H. Xu, H. A. Toliyat, and L. J. Petersen, "Five-phase induction motor drives with DSP-based control system," *IEMDC 2001 - IEEE Int. Electr. Mach. Drives Conf.*, pp. 304–309, 2001.

[5] M. H. Holakooie, M. Ojaghi, and A. Taheri, "Modified DTC of Six-Phase Induction Motor With a Second-Order Sliding-Mode MRAS-Based Speed Estimator," *IEEE Trans. Power Electron.*, vol. 8993, no. c, pp. 1–1, 2018.

[6] K. P. P. Rao, B. K. Veni, and D. Ravithej, "Five-Leg Inverter for Five-Phase Supply," *Int. J. Eng. Trends Technol.*, vol. 3, no. 2, pp. 144–152, 2012.

[7] H. Vahedi, P. A. Labbé, and K. Al-Haddad, "Sensor-Less Five-Level Packed U-Cell (PUC5) Inverter Operating in Stand-Alone and Grid-Connected Modes," *IEEE Trans. Ind. Informatics*, vol. 12, no. 1, pp. 361–370, 2016.

[8] H. Vahedi, A. A. Shojaei, L. Dessaint, and K. Al-haddad, "Reduced DC Link Voltage Active Power Filter Using Modified PUC5 Converter," *IEEE Trans. Power Electron.*, vol. PP, no. 99, 2017.

[9] A. Iqbal and E. Levi, "Space vector PWM techniques for sinusoidal output voltage generation with a five-phase voltage source inverter," *Electr. Power Components Syst.*, vol. 34, no. 2, pp. 119–140, 2006.

[10] C. Tan, D. Xiao, J. E. Fletcher, and M. F. Rahman, "Analytical and Experimental Comparison of Carrier-Based PWM Methods for the Five-Phase Coupled-Inductor Inverter," *IEEE Trans. Ind. Electron.*, vol. 63, no. 12, pp. 7328–7338, 2016.

[11] K. Shirabe *et al.*, "Advantages of high frequency PWM in AC motor drive applications," *2012 IEEE Energy Convers. Congr. Expo.*, pp. 2977–2984, 2012.

[12] M. Tariq, M. T. Iqbal, M. Meraj, A. Iqbal, A. I. Maswood, and C. Bharatiraja, "Design of a Proportional Resonant Controller for Packed U Cell 5 Level Inverter for Grid-Connected Applications," pp. 3–8, 2016.

[13] K. S. Aher and A. G. Thosar, "Modeling and Simulation of Five Phase Induction Motor using MATLAB / Simulink," vol. 6, no. 5, pp. 1–8, 2016.

[14] A. Iqbal *et al.*, "Modeling , Simulation and Implementation of a Five-Phase Induction Motor Drive System," 2010.

[15] L. Tan, B. Wu, M. Narimani, D. Xu, and G. Joos, "Multicarrier-Based PWM Strategies with Complete Voltage Balance Control for NNPC Inverters," vol. 46, no. c, pp. 1–10, 2017.